

Brain Tumor Area Segmentation of MRI Images

Behnam Kiani Kalejahi

*Faculty of Engineering and Applied Sciences,
Khazar University, Azerbaijan
bkiani@khazar.org*

Abstract

Accurate and timely detection of the brain tumor area has a great impact on the choice of treatment, its success rate, and following the disease process during treatment. The existing algorithms for brain tumor diagnosis have problems in terms of good performance on various brain images with different qualities, low sensitivity of the results to the parameters introduced in the algorithm, and also reliable diagnosis of tumors in the early stages of formation. In this study, a two-stage segmentation method for accurate detection of the tumor area in magnetic resonance imaging of the brain is presented. In the first stage, after performing the necessary preprocessing on the image, the location of the tumor is located using a threshold-based segmentation method, and in the second stage, it is used as an indicator in a pond segmentation method based on the marker used. Placed. Given that in the first stage there is not much emphasis on accurate detection of the tumor area, the selection of threshold values over a large range of values will not affect the final results. In the second stage, the use of the marker-based pond segmentation method will lead to accurate detection of the tumor area. The results of the implementations show that the proposed method for accurate detection of the tumor area in a large range of changes in input parameters has the same and accurate results.

Keywords: Brain tumor, MRI images, Tumor segmentation, Brain MR Images.

Introduction

A brain tumor is a hard, solid neoplasm inside the brain or the central spinal canal. In simpler terms, a brain tumor is an abnormal mass in the brain that may be cancerous (malignant) or noncancerous (benign) in nature. The degree of threat of a tumor depends on a set of factors such as type, location, size, life, and how it spreads and develops. The brain is completely covered by the skull. This makes rapid and

early detection of brain tumors possible only if paraclinical instruments and appropriate diagnostic devices are available to assess the condition of the intracranial cavity in the early stages of tumor formation. Even with these tools, it is very difficult to accurately diagnose brain tumors due to their variety of shapes, sizes, and appearances. In addition, in most cases, brain tumors are diagnosed in the advanced stages of the disease and when its presence causes unexplained signs and symptoms in the patient. Magnetic resonance imaging is commonly used to visualize details of the internal structure of the body. In this imaging method, differences in the magnetic properties of the fabric are used to form the image. The magnetic moment of the nucleus of some elements in the presence of a strong magnetic field is also aligned with it. The amplitude of the received signal in magnetic resonance imaging depends on two factors, the density of the protons and the rest times T1 and T2. The rest time T1 is the temporal period at which 63% of the longitudinal magnetic moment of a proton returns from the direction perpendicular to the field to the parallel direction of the field after excitation. The resting time of T2 is also the length of time that the transverse magnetic moment of a proton decreases to 37% of its initial value after excitation. Pathological processes increase T1 and T2 rest periods. Compared to the natural textures around them in T1-Weighted images, the signal amplitude is lower (darker image) and T2-Weighted images produce a larger signal amplitude (brighter image). According to the above, it is possible to diagnose a brain tumor with a bandage image in terms of uniformity of light intensity. Manually isolating the tumor area in images of magnetic resonance imaging of the brain is a time-consuming and quite difficult process. Today is progressing image segmentation algorithms have also been enabled to automatically detect brain tumors. Automated brain tumor detection methods, while reducing operator work and human error, also make it easy to store tumor growth status during treatment (Faisal et al. 2013). However, due to the variety in the shape, size, and appearance of tumors, it is very difficult to achieve high accuracy in detecting tumors in a wide range of images. Also, the proper performance of many of the algorithms presented for the segmentation of magnetic resonance imaging of the brain depends on the proper selection of the input parameters of the algorithm as an example.

The KIFCM method presented in (Faisal et al., 2013), plays an important role in the exact banding of the tumor in the magnetic resonance imaging of the brain. In addition, for selecting the values of the input parameters, a large range of values cannot be selected by the user. For example, in (Harati et al., 2011) the user may not even be mentally aware of the appropriate value of the parameter used in the algorithm, and in (El-Dahshan et al., 2014.) according to the author the success of using the PCNN method to segment to properly adjust various network parameters such as communication parameter, (β) thresholds, (Θ) The disappearance time constants ($\alpha\theta$) and the internal connection matrices M and W depend on the fact that

the user may not have a reasonable amount of the parameters used in this method. In this paper, an effective two-step algorithm for accurate segmentation of the brain tumor area in magnetic resonance imaging is presented. The proposed two-stage segmentation method is organized in such a way that in the first stage the ability to reduce the sensitivity of the algorithm results in the selection of parameters and thus increase the range of selectable numbers for the parameters is available and in the second stage to improve the results. In the first stage, a threshold-based segmentation method was used to locate the tumor, and in the second stage, a pond-based segmentation method was used to accurately detect the shape of the tumor (Guo et al., 2012). The results of the implementation show that the proposed two-step method has a precise function in tumor detection on a large range of selected input parameters and on a wide range of magnetic resonance imaging images of the brain.

Related Works

The segmentation of the image is done by different methods. Clustering is one of the common methods in this field. In (Abdel-Maksoud et al., 2015), a combined clustering system is presented which includes the three main stages of preprocessing, clustering, extraction, and contouring. The image obtained from the preprocessing stage is clustered by the K-means clustering technique with the Fuzzy C-means algorithm and then by the thresholding method.

The cluster, the area of the tumor is extracted, or in other words, the initial location. In the last step, the leveling algorithm is applied to the image and provides a more accurate segmentation. The dependence of the output on the parameters such as the number of clusters, maximum replication, and the closing parameter are the disadvantages of this method. In Reference (Harati et al., 2011), Vida Herati et al. Have proposed a method based on an improved fuzzy communication algorithm for brain tumor segmentation (Havaei et al., 2017). In this method, first, a point of seed is automatically selected from inside the tumor. For adjacent pixels, the amount of brightness based on the sum of the mean intensity is corrected in a certain range in the original image and the main image derivative to improve the performance of the fuzzy communication algorithm at weak limits. In the next step, the amount of fuzzy communication for each new pixel is calculated based on comparing the similarity of that pixel with the characteristics of the tumor area. Finally, the tumor site is extracted by astringency. The similarity index for this method is 89.92%. In (El-Dahshan et al., 2014), FPCNN pulsed buccal neoplasm feedback has been used to define the area in question by segmentation of MRI images of the brain. Neural network feedback with pulse coupling consists of three main parts: acceptance,

modulation, and pulse generation. The main difference between this model and PCNN is that the input is replaced by the input drive and output feedback to modify the input. According to the author, the success of using the FPCNN method for segmentation depends on the proper adjustment of various network parameters such as connection parameters (β), thresholds (θ), time-disappearing constants ($\alpha\theta$) and internal connection matrices M and W .

In (Sachdeva et al., 2012), a content-based active boundary model is used for tumor segmentation. In this system, the primary cantilever is first radiologically marked in the tumor area and then the tissue properties and severity are estimated and using it, the tumor is formed and energy is formed. External contour deformation is used. In the next step, the static motor field and the dynamic motor field are generated to guide the macro center to the tumor margins. Contour deformation is stopped by limiting the number of repetitions or reaching fixed criteria. Not completely automatic is one of the problems of this method. Segmentation and diagnosis of tumor lesions and stroke have also been implemented by optimization algorithms.

Noshin Nabizadeh et al. (Nabizadeh et al., 2014) used a histogram-based gravity optimization algorithm. This algorithm is divided into two separate sections, including the histogram-based brain segmentation algorithm and the n-dimensional optimal optimization algorithm. This algorithm uses histogram-based techniques to determine the initial set of brain segments, and then apply the gravitational optimization algorithm to reduce the number of sections to the user's desired number and finally use the threshold to identify waste Tumor or stroke. Appropriate determination of input parameters such as the selection of the number of parts of the brain, the number of first-generation, the number of repetitions, and the like are some of the problems of this method. Also, in (Arakeri and Reddy, 2013), a combination of wavelet analysis and modified FCM MFCM is suggested for tumor segmentation. In this system, first, the removal of the skull is done by the method of astringency and preservation of the largest connected component, in the next stage of properties, the weave is revealed by the application of discrete wavelet transform. In the next part, the number of peaks in the brain histogram is used to detect the presence of a tumor in MRI images. The image containing the tumor is then clustered into four sections: CSF, GM, WM, and abnormal, by the MFCM algorithm, and the cluster with the highest value of the cluster center is selected as the abnormal region. Finally, the number of peaks in the histogram of the abnormal area is used to determine the presence of a swollen area associated with the tumor. If there is a swollen area, the abnormal area is clustered into two tumor clusters and the swollen area by the MFCM algorithm. This study seeks a fully automated method with low sensitivity to input parameters that can accurately detect the tumor area.

Implementation of the proposed method

The proposed method includes four stages of initial preprocessing, skull removal, marking positioning using the threshold-based segmentation method, and finally marker-based pond conversion. In this section, in addition to introducing the data set to be used, the implementation details of each of these steps are stated.

Data collection

In this paper, the BRATS2018 standard data set has been used (<http://www2.imm.dtu.dk/projects/BRATS2018/>). This dataset contains FLAIR, T2, T1, and T1C images for each patient.

Pre-processing

The initial preprocessing step includes image normalization in terms of size and brightness values, noise cancellation and image sharpening. At this stage, the input MRI image is first converted to a gray surface image, the brightness values between zero and one are normalized and the image dimensions are changed to 250×250 . Noise removal is done using the middle filter. To repair the details lost during the noise removal and sharpening of the brain image, the image details are extracted using a high-pass filter and added to the original image.

The skull, skin, and other non-brain tissues in some methods may be misaligned or at least increase processing time due to their strong resemblance to the brain structure, so they need to be removed. In this system, skull removal is performed by a method based on measuring the properties of the image areas.

This method works in such a way that initially the average brightness of the image is calculated and a fuzzy system specifies the threshold value for the image. By applying this amount of threshold on the image, the tumor tissue and the skull (as two attached components) are identified. Then a set of different properties is calculated for each connected component (object) in the binary image, and based on these properties, an attached component is selected as the skull component. In other words, any component attached to an image that has certain properties is known as a skull and is removed. For example, the number of pixels in each component will have a "hard" property, which indicates the percentage of a region being thicker, for the skull component. Therefore, the largest area with low stiffness can be considered as a component of the skull.

Threshold-based segmentation

Thresholding is a simple but effective technique for image segmentation. The thresholding technique is based on dividing the image into separate regions (object and background) in such a way that one part contains pixels with a higher intensity equal to or equal to the threshold value, and the other part contains pixels with a smaller value. It will be the amount. Finding the right threshold value to separate the desired object from the background is an important step in processing the machine image and vision (Zhou, 2018).

If T is the value of the threshold and $f(x, y)$ the brightness of the point (x, y) in the gray image, the threshold image is calculated as follows:

$$g(x, y) = \begin{cases} 1 & f(x, y) \geq T \\ 0 & f(x, y) < T \end{cases}$$

In order to perform accurate thresholding and to obtain a binary image that includes the desired details, parallel thresholding has been used. This technique uses two methods of fuzzy thresholding and adaptive thresholding in parallel. In the first method, the threshold value is selected through a fuzzy system in proportion to the intensity of the image. In the fuzzy thresholding method, a fuzzy system with three trapezoidal membership functions for low, medium, and high modes receives the average light intensity of the image as input and the threshold value as output. The fuzzy rules used are such that the threshold value is selected from the low, medium, and high values for the threshold value depending on the average value of the image, which is low, medium, or high, respectively (Ain et al., 2014).

Adaptive thresholding is also applied to the image based on the mean value and the variance of the image according to Equation (Jaccard, 1912).

$$f_{Th}(x, y) = \frac{1}{e^{\frac{(f(x, y) - Mean(f(x, y)))^2}{Var(f(x, y))}}}$$

In the two methods mentioned, the threshold value is determined automatically and is obtained from the heart of the image. One advantage of using the parallel thresholding technique is that if the threshold value is set incorrectly and the segmented image is inappropriate, another method corrects the final image using sharing. But the correction itself consists of two modes: the first mode occurs when, for example, the first method fails to determine the appropriate threshold value and divides the tumor area larger than its actual size, in which case the second method

Properly operated, the output image is modified by sharing two images (Chang et al., 2018.).

But in the second case, if the area of the tumor is smaller than the actual size of that section, in the output image, the size of the tumor will also be smaller. The final will not be created. Because the output of the parallel thresholding stage is used as an indicator for the pond conversion algorithm in the final stage (Rezaei et al., 2017.).

In fact, the cause of error at this stage is the segmentation of the tumor area is larger than the actual size because it will cause the pond conversion algorithm to be mistaken and the smaller segmentation of the tumor area will not cause a problem in the final exit. In other words, the implementation of this step is done with the aim of reducing the dependence of the algorithm on the selection of input parameters (including threshold values) and accuracy is not a priority at this stage. Using the pond segmentation method based on the marker will then be used to accurately detect the tumor area (Yang et al., 2018.).

The pond conversion algorithm is a zone-based segmentation method that performs segmentation based on the image intensity. The visual idea of this method is taken from geography and immersed by imagining an image as a three-dimensional map.

This map is implemented in a lake of water with holes drilled in the local minima of this map. Water rises in different ponds with the same rate of increase and reaches the same points. Vertical dams are placed at these points to prevent the pools from joining water continuously. After the highest point of the map is submerged in water, the dams divide the map into separate areas. These dams are in fact the same lines they are ponds (Zijdenbos et al., 1994; Jaccard., 1912).

To zoning the image using the pool conversion, first, the intensity of the image brightness gradient is calculated and then the pool conversion is applied to it. In the light intensity gradient image, the values for the edge points are higher than the values for the other points. Therefore, the pond lines are located around the edges. This is suitable for image zoning. The pond conversion algorithm, in addition to all its advantages, suffers from a major problem of additional bandwidth, which occurs due to a large number of local minimums and causes the number of detected areas to be larger than the number of objects. In the proposed system, in order to eliminate the effect of most of the bandage zone, the method of segmentation of the pool-based indicator has been proposed (Kong et al., 2018.). The area of the tumor located in the threshold stage is determined in parallel with the application of a series of minimization operations as internal markers (tumor). Black areas are also considered as backgrounds, but ideally, we do not want the background markers to be too close to the edges of the objects we are trying to segment (internal markers). This will be

done by thinning the background by calculating SKIZ from the binary image foreground (Alex et al.,2017.).

Evaluation

In this paper, the threshold value and σ value in the step of calculating the gradient are considered as input parameters and the effect of changes in these parameters on the output results is investigated. The results of the proposed algorithm with the application of different threshold values are shown in Figure 1

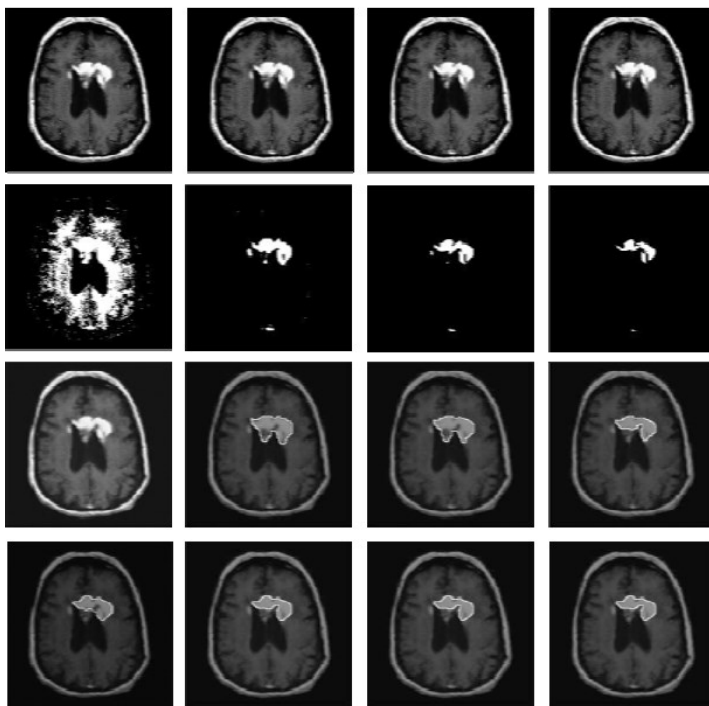


Figure 1. The results of the proposed algorithm by applying different threshold values. (a) Original image. (b) Threshold output. (c) Results of the single-indicator pool-based algorithm. (d) The results of the proposed algorithm

In this system, the selection of the threshold value in the parallel thresholding stage was completely automatic, but to evaluate the system and check the sensitivity of the algorithm results to the input parameters, the threshold value in the parallel thresholding stage is about 0.3 to large. 0.9 has been selected. As can be seen, by

changing this parameter in a relatively large body and the inappropriate output of the parallel threshold stage, the output of the proposed algorithm has the least change and still accurately performs the banding of the tumor area.

Also, to approximate the image gradient, image convolution with a Gaussian-oriented filter has been used. In this two-dimensional symmetric filter, the parameter σ is the standard deviation of the Gaussian function. σ determines the width of Gauss and its increase is removed by removing more details. The effect of changes in this parameter on the output results has also been investigated.

Similarly, the value of the parameter σ in the image gradient calculation step is changed in the range of 0.5 to 3, which is a large range of values for the parameter σ , to investigate the effect of changes in this parameter on the output results. It is observed that with the changes of σ , the output results of the proposed algorithm have the least change, and also the banding of the tumor area is done properly.

To further ensure the proper performance of the proposed algorithm, a quantitative evaluation of the results of the algorithm for the standard data set has also been performed. In order to quantitatively evaluate the performance of the proposed method, T1C images of the BRATS 2012 dataset and its reference images were used. The following five criteria were used to quantitatively compare the location of the extracted tumor and its position in the reference images stored as binary.

$$\begin{aligned}
 \text{Sensitivity} &= \frac{TP}{TP + FN} \times 100 \\
 \text{Specificity} &= \frac{TN}{TN + FP} \times 100 \\
 \text{Accuracy} &= \frac{TP + TN}{TP + TN + FN + FP} \times 100 \\
 \text{Dice Similarity Score} &= \frac{2(TP)}{2(TP) + FN + FP} \times 100 \\
 \text{Jaccard Similarity Index} &= \frac{TP}{TP + FN + FP} \times 100
 \end{aligned}$$

In the above equation, FP, TN, TP, and FN, respectively, represent the number of pixels that have been correctly identified as part of the tumor, the number of pixels that have been correctly identified as the year texture, and the number of pixels that have been incorrectly identified as Part of the tumor has been identified and the number of pixels that have been mistakenly identified as healthy tissue.

Dice's similarity score actually measures the ratio of properly segmented tumor tissue to the total area of tumor tissue in both the reference and segmented images. DSS values range from zero to one, and the proximity of this value to an indicator

The segmentation is more accurate (Zijdenbos et al., 1994). Also, the value of one for the Jacquard similarity index (Jaccard, 1912) indicates the existence of complete similarity between the two sets and the value of zero indicates the non-similarity between the two sets. The two Dice similarity score criteria and the Jaccard similarity index show both degrees of overlap between the actual tumor and the extracted tumor. Figure 2 shows the results of this implementation. The performance of the proposed algorithm in the brain tumor segmentation for the 2012 BRATS dataset is shown in Table 1.

Table 1. Results of tumor segmentation by the proposed algorithm on the images shown in Figure 7 of the BRATS 2012 dataset

Image number	DSS	Sensitivity	Specificity	Accuracy	JSI
1	95/83	94/85	99/89	99/70	92/00
2	96/22	98/91	99/82	99/79	92/72
3	90/68	96/77	99/91	99/89	91/08
4	94/53	96/82	99/92	99/89	89/63
5	93/89	98/00	99/81	99/78	88/48
6	95/22	97/53	99/88	99/84	90/88

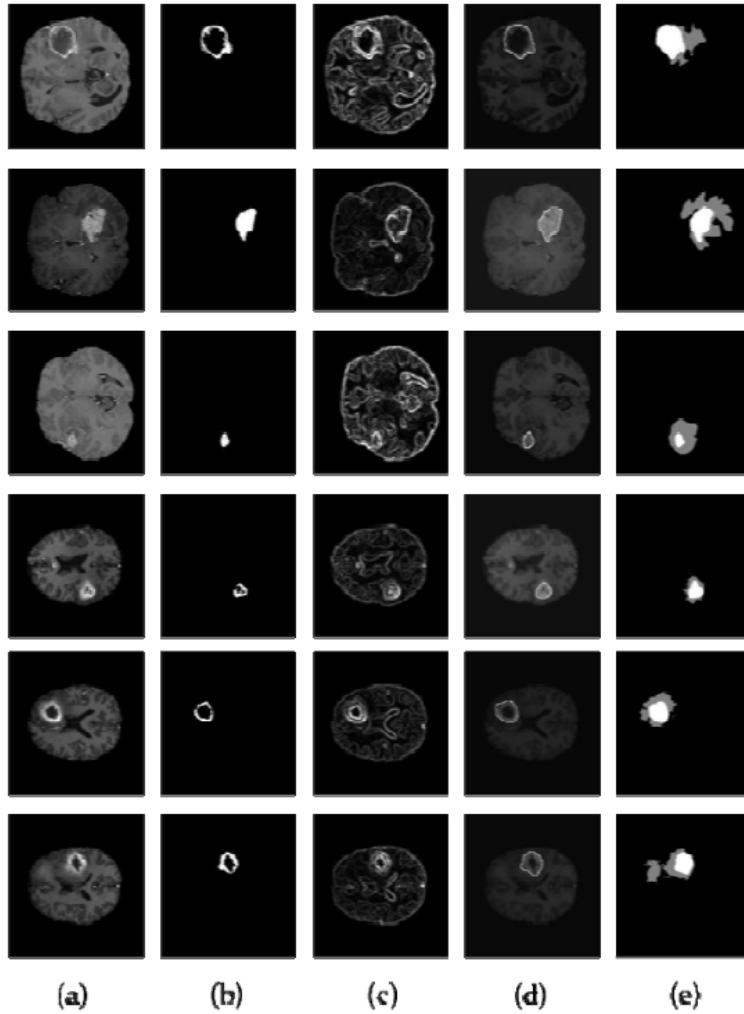


Figure 2. Results of implementation of the proposed method on the data set BRATS 2012

(a) Original image (b) Parallel threshold output with morphological processing (c) Rotation of the original image (d) Tumor area (e) Reference image

Conclusion

The two-stage segmentation algorithm proposed in this paper is a combination of two threshold-based segmentation methods and an indicator-based pond segmentation method. Each of these methods alone has one drawback. The results of the threshold-based segmentation method are highly dependent on the choice of

input parameters, and for each image, a different threshold value is needed from the other image, in other words, it is not an automated method. The pond section also has the problem of creating additional areas.

However, the reason for choosing these two methods is that they are able to cover each other's weaknesses. Threshold-based segmentation the problem of additional areas covers the pond sealing section and the pond sealing section covers the problem of low-precision threshold-based segmentation. In addition, because in the threshold-based segmentation method the goal is to locate the tumor area and not to accurately detect it, the input parameters of this step can be selected in a large range of values.

Also, the proposed algorithm is able to provide accurate output for tumors of different shapes, sizes and appearances in various images. This is despite the fact that the input parameters of the algorithm were fixed for all images. The implementations show that the proposed hybrid algorithm, in addition to being automated, has yielded accurate results on a wide range of images.

References

- Abdel-Maksoud, E., Elmogy, M., and Al-Awadi, R.,** (2015) "Brain tumor segmentation based on a hybrid clustering technique," *Egypt. Informatics J.*
- Ain, Q., Jaffar, M. A., and Choi, T. S.** (2014) "Fuzzy anisotropic diffusion-based segmentation and texture-based ensemble classification of brain tumor," *Appl. Soft Comput.*, vol. 21, no. 2014, pp. 330–340, Aug.
- Alex V., Safwan M. Krishnamurthi,** (2017) Brain tumor segmentation from multi modal MR images using fully convolutional neural network, *Medical Image Computing and Computer Assisted Intervention - MICCAI* 1–8.
- Arakeri, M. P. and Reddy, G. R. M.,** (2013) "Computer- aided diagnosis system for tissue characterization of brain tumor on magnetic resonance images," *Signal, Image Video Process.*, Apr.
- Chang H., Lu J., Yu F., Finkelstein A.,** (2018) Pairedcyclegan: asymmetric style transfer for applying and removing makeup. *IEEE Conference on Computer Vision and Pattern Recognition (CVPR).*
- El-Dahshan, E. S. a., Mohsen, H. M., Revett, K., and Salem, A. B. M.** (2014) "Computer-aided diagnosis of human brain tumor through MR I: A survey and a new algorithm," *Expert Syst. Appl.*, vol. 41, no. 11, pp. 5526–5545, Sep.
- Faisal, A., Parveen, S., Badsha, S., Sarwar, H., and Reza, A. W.,** (2013) "Computer assisted diagnostic system in tumor radiography," *J. Med. Syst.*, vol. 37, no. 3, pp. 1-10.
- Guo, X., Tang, C., Zhang, H., and Chang, Z.,** (2012) "Automatic thresholding for defect detection," *ICIC Express Lett.*, vol. 6, no. 1, pp. 159–164.

- Harati, V., Khayati, R., and Farzan, A.,** (2011) “Fully automated tumor segmentation based on improved fuzzy connectedness algorithm in brain MR images,” *Comput. Biol. Med.*, vol. 41, no. 7, pp. 483–492.
- Havaei M., Davy A., Warde-Farley D. et al.** (2017) “Brain tumor segmentation with deep neural networks,” *Medical image analysis*, vol. 35, pp. 18–31.
- Jaccard P.** (1912) “The distribution of the flora in the alpine zone,” *New Phytol.*, vol. XI, no. 2, pp. 37–50.
- Kong X., Sun G., Wu Q., Liu J., Lin F.,** (2018) Hybrid pyramid U-Net model for brain tumor segmentation, in: *International Conference on Intelligent Information Processing*, Springer, pp. 346–355.
- Multimodal Brain Tumor Segmentation Challenge, Web:** (2012) data available at <http://www2.imm.dtu.dk/projects/BRATS2012/>
- Nabizadeh, N., John, N., and Wright, C.,** (2014) “Histogrambased gravitational optimization algorithm on single MR modality for automatic brain lesion detection and segmentation,” *Expert Syst. Appl.*, vol. 41, no. 17, pp. 7820–7836, Dec.
- Rezaei M., Harmuth K., Gierke W., Kellermeier T., Fischer M., Yang H., Meinel C.,** (2017) A conditional adversarial network for semantic segmentation of brain tumor, in: *International MICCAI Brainlesion Workshop*, Springer, pp. 241-252.
- Sachdeva, J., Kumar, V., Gupta, I, Khandelwal, N, and Ahuja, C. K.,** (2012) “A novel content- based active contour model for brain tumor segmentation,” *Magn. Reson. Imaging*, vol. 30, no. 5, pp. 694–715.
- Yang X., Xu Z., Luo J.,** (2018) Towards perceptual image dehazing by physics-based disentanglement and adversarial training, *The Thirty-Second AAAI Conference on Artificial Intelligence (AAAI-18)*.
- Zhou, C., Chen, S., Ding, C., Tao, D.:** (2018) Learning contextual and attentive information for brain tumor segmentation. In: *International Conference on Medical Image Computing and Computer Assisted Intervention (MICCAI 2018)*. *Multimodal Brain Tumor Segmentation Challenge (BraTS 2018)*. *BrainLes 2018 workshop*. LNCS, Springer.
- Zijdenbos A.P., Dawant B. M., Margolin R. A., and Palmer A. C.** (1994) “Morphometric analysis of white matter lesions in MR images: method and validation.,” *IEEE Trans. Med. Imaging*, vol. 13, no. 4, pp. 716–24.